CHEMISTRY
AN ASIAN JOURNAL
ACES
COMMUNICATION

DOI: 10.1002/asia.201300399

A Simple Fabrication of Interconnected CuO Nanotube Electrodes for High-Performance Lithium-Ion Batteries

Jung-In Lee, Sinho Choi, and Soojin Park*[a]

Lithium-ion batteries (LIBs) are desirable energy storage devices with numerous applications, such as portable electronics, electric vehicles, utility grids, and energy-storage systems, due to their energy density, power performance, and cycling life.[1–3] Current commercial LIBs consisting of a $LiCoO_2$ cathode and a graphite anode possess limited specific capacity and energy density.[1] Thus, further development of alternative active materials with higher specific capacity is essential. In particular, the development of anode materials with a high capacity is urgent since anode materials have several drawbacks, such as a large volume change and unstable cycling.[4–8]

Among the various anode materials, copper oxide (CuO) has been considered as a promising candidate owing to its high capacity (ca. 670 $mAh\,g^{-1}$), low cost, and abundance.[9,10] The electrochemical process of the CuO electrode, based on a maximum uptake of 2 Li per CuO, proceeds in the following reaction: $CuO+2Li^{+}+2e^{-}\leftrightarrow Cu+Li_2O$.[9,10] However, pure CuO electrodes have shown a poor cycling life and a low capacity at high rates, which may be mainly attributed to its low conductivity and structural collapse due to a large volume change during the cycling process.

To solve these critical problems, a number of strategies have been developed by designing various nanostructures (e.g., nanowires, nanotubes, hollow structures, hierarchical structuring, etc.) and surface coating.[11–15] Especially, since hollow structured electrodes exhibit a high surface area, easy accessibility of electrolytes and Li^{+} ions, and buffering of a large volume change during cycling, hollow and/or nanotubular structuring is an effective method to make high-performance LIB anodes.[4,16] A template-based process, etching process, and Kirkendall-based approach have been used to prepare such novel structures.[11–15] As another strategy, active materials that are strongly attached to the metallic current collector have several advantages, such as the introduction of electronic pathways allowing for effective charge transport and a binder/conducting additive-free system.[17,18]

Herein, we report a simple but effective fabrication process to make a high-performance CuO nanotube anode that is strongly attached to the stainless steel (SS) current collector. Alkylamine-stabilized Cu nanowires were synthesized by a hydrothermal process. Subsequently, a stable suspension of as-synthesized Cu wires was spin-coated on the SS surface, followed by a thermal annealing in air to remove the alkylamine surfactant and to prepare interconnected CuO nanotube networks. These CuO nanotube anodes exhibit high-performance electrochemical properties, including a high specific capacity (ca. 635 $mAh\,g^{-1}$), stable cycling (capacity retention of $>99\,\%$ after 50 cycles), and excellent rate capabilities (315 $mAh\,g^{-1}$ at 20 C rate).

Copper nanowires were synthesized by a simple chemical reaction using a long alkylamine, which can act as a non-ionic surfactant and a reducing agent. The advantage of this process is that it does not require a catalyst or porous template to grow the nanowire. Primary amines can reduce copper(II) ions to copper metal,[19] and subsequently, as-prepared copper seeds lead to the growth of nanowires through the Ostwald ripening process.[20,21] In addition to the use of alkylamine as a reducing agent, a surfactant with a long alkyl chain can act as a shape-controlling soft template during the ripening process.[20,21] It is well known that a long alkylamine dissolves in water at temperatures well above 120 °C and that subsequently the amino groups are bound with Cu^{II} cations in an aqueous solution.[22] Copper(II) cations were transferred from the aqueous phase to the interface between the long alkyl chain and the aqueous phase, and the Cu seeds, which constitute the source material for growing Cu nanowires, were formed through reduction by the amino group. Alkylamines that have long alkyl chains form reverse micelles in water, and the interlayers of the micelles can be used as scaffolds or templates to prepare nanowires.[23,24]

Figure 1 shows scanning electron micrographs (SEM) of copper nanoparticles and nanowires grown via the hydrothermal reaction of three different alkylamines (*n*-decylamine (C10-NH_2), *n*-tetradecylamine (C14-NH_2), and *n*-octadecylamine (C18-NH_2, 2 mM each)) with copper chloride ($CuCl_2$, 12.5 mM) at 160 °C for 72 hours. The average diameters of nanowires prepared from C10-NH_2, C14-NH_2, and C18-NH_2 molecules were approximately 850 nm, 250 nm, and 100 nm, respectively (Figure 1). Since an alkylamine

[a] J.-I. Lee, S. Choi, Prof. S. Park
Interdisciplinary School of Green Energy
Ulsan National Institute of Science and Technology (UNIST)
Ulsan 689-798 (Korea)
Fax: (+82) 52-217-2909
E-mail: spark@unist.ac.kr

Supporting information for this article is available on the WWW under http://dx.doi.org/10.1002/asia.201300399.

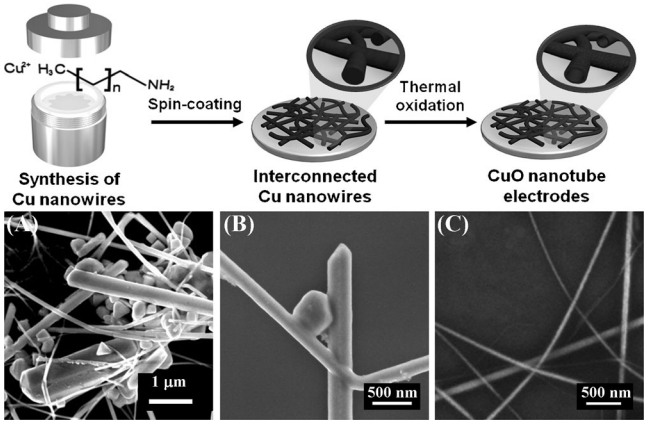

Figure 1. Top: Schematic illustration showing the preparation of interconnected CuO nanotubes through thermal oxidation of Cu nanowires. Bottom: SEM images showing copper particles and nanowires synthesized via a hydrothermal reaction of $CuCl_2$ and (A) *n*-decylamine, (B) *n*-tetradecylamine, and (C) *n*-octadecylamine.

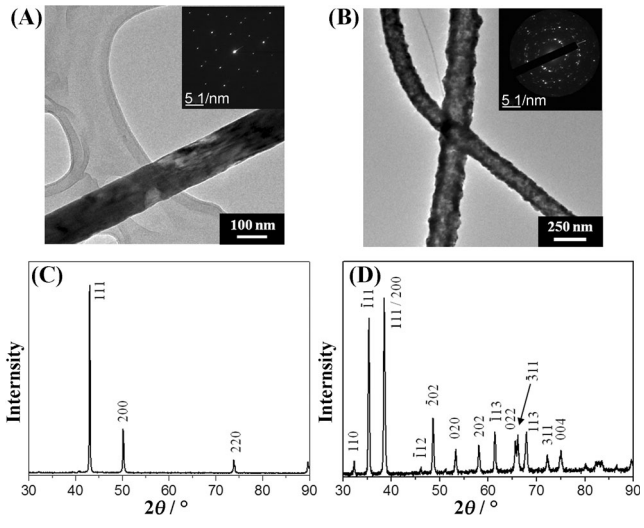

Figure 2. TEM images of Cu nanowires prepared from C18-NH_2 (A) and CuO nanotubes (B) prepared via thermal oxidation at 400 °C for 1 h. The corresponding XRD patterns of Cu (C) and CuO (D) indicate face-centered cubic and monoclinic structures, respectively.

with a long alkyl chain is bulky as compared to that with a short alkyl chain, it limits the growth of Cu nanoparticles in the nucleation stage, thus leading to the formation of nanowires with a smaller diameter. Similar results were observed in cases of spherical nanoparticles that were prepared from surfactants with several different molecular sizes.[20] There were similar contents to the nanowires and microcrystals found when the C10-NH_2 molecules were used. It seems that C10-NH_2 with a short alkyl chain was less effective to protect the aggregation of Cu nanoparticles.

Next, the average diameters of the nanowires prepared from alkylamines with different alkyl chain lengths and at different reaction temperatures were determined. All Cu nanowires, irrespective of the alkylamine used, exhibited high-quality single-crystalline characteristics and grew along the [1$\bar{1}$0] plane, as seen in selected area electron diffraction (SAED) patterns and high-resolution transmission electron microscopy (HR-TEM) images (Supporting Information, Figure S1).

The Kirkendall effect, a classic phenomenon in metallurgy,[25–27] was recently applied to make nanotubes[28] or hollow spherical nanocrystals.[29] Typically, when metal nanoparticles are exposed to oxygen at high temperature, a diffusivity difference of metal cations and anions takes place. Since outward diffusion of the metal cations is much faster than the inward diffusion of the anions, hollow spherical metal-oxide nanoparticles are formed. In a similar manner, when the pure Cu nanowires were thermally oxidized at 400 °C for 1 hour in air, metallic Cu was transformed to copper oxide (CuO), and the diameter increased.[30] Compared to complex chemical methods, the thermal oxidation process is much faster and more convenient. The surface of pure Cu nanowires (prepared from C18-NH_2) reacts continuously with oxygen in air at certain temperatures, and subsequently the Cu cations move toward the surface of the nanowires, resulting in the formation of CuO nanotubes (Figure 2B). The formation of as-synthesized CuO nanotubes was confirmed by analysis of the XRD patterns (Figure 2D). The peaks observed correspond to those of monoclinic (*C*2/*c*) CuO (JCPDS 45-0937, lattice constant, $a = 4.684$ Å, $b = 0.343$ Å), thereby indicating that the thermal oxidation process was successfully carried out. As reported previously by Nakamura et al.,[27] Cu nanowires were transformed into oxide nanotubes with uniform inner and outer diameters.

The diameters of CuO nanowires can be tuned by varying the thermal annealing time in air. After the Cu nanowires were thermally oxidized at 400 °C for 30 min, 1 h, and 2 h, respectively, SEM images were taken for 30 samples prepared at each annealing time to obtain average diameters. At annealing times of 0.5 and 1 h, the diameters of CuO wires were 1.3 and 1.7 times larger, respectively, than that of the as-prepared copper wires. At the annealing time of 2 h, the growth of CuO wires in diameter reached a plateau (Figure S2, Supporting Information).

We then went on to fabricate interconnected CuO nanotube electrodes that strongly adhered to an SS current collector. To this end, a stable suspension of alkylamine-decorated Cu nanowires in water was spin-coated on SS foil and dried. This process was repeated 10 times in order to cover the surface of the SS foils. Afterwards, the Cu nanowire-coated SS foils were thermally oxidized at 400 °C for 1 h to yield CuO nanotubes on the SS foil, while organic layers were completely degraded under these conditions. SEM images of the spin-coated Cu nanowires and as-synthesized CuO nanotube electrodes are shown in Figures S3 and S4 in the Supporting Information. The CuO nanotubes prepared by thermal oxidation of Cu nanowires generated in the presence of C14-NH_2 and C18-NH_2 can be clearly observed (Figure S4b,c). Furthermore, cross-sectional images of the CuO nanotubes obtained by focused ion beam show the hollow structures that resulted from the Kirkendall effect (Figure S5, Supporting Information).

The CuO nanotube electrodes that are strongly attached to the SS foils may offer the following advantages compared to those fabricated by the conventional slurry process. First, the facile solution-based process (spin-coating method) can finely control the thickness of the electrode. Second, no binder or conductive materials (e.g., super P carbon black) are required due to a strong interaction between the CuO nanotubes and the SS foils. Third, the CuO nanotubular structure can accommodate the large volume changes during the lithium insertion and extraction process. Fourth, the interconnected structure between the CuO nanotubes and void spaces can improve the electron transfer and the accessibility of lithium ions and electrolytes.

The CuO nanotube electrode made from C18-NH_2 was then employed as the anode active material in LIBs. Figure 3A shows the voltage profiles of the CuO nanotube electrodes at a rate of 0.1 C in the range of 0.005–3.0 V with increasing number of cycles. In the first cycle, three typical sloping potential ranges are observed at 2.25–1.8, 1.4–1.0, and 1.0–0.02 V versus Li^+/Li for the lithium insertion.[7] The discharge and charge capacity of the CuO nanotubes in the first cycle was 808 and 582 mAh g^{-1}, respectively, indicating a coulombic efficiency of 72%. The low coulombic efficiency of the CuO electrode is attributed to the conversion reaction process of metal oxides, and subsequent cycles show a significantly enhanced coulombic efficiency.[31] After 50 cycles, the reversible charge capacity was 635 mAh g^{-1}, corresponding to a capacity retention of nearly 100% compared to the initial capacity. These results indicate that the nanotubular structure of CuO acts as an efficient buffer for a large volume change during cycling and that the CuO nanotubes remained strongly attached to the SS foils and did not detach from the current collector. Similarly, CuO nanotube electrodes made from C10-NH_2 and C14-NH_2 displayed a highly stable cycling retention (Figure S6, Supporting Information). However, the initial coulombic efficiencies of both electrodes were quite low, due to the formation of large aggregates of CuO during cycling, compared to the CuO nanotube electrode made from C18-NH_2 (Figure S7, Supporting Information).

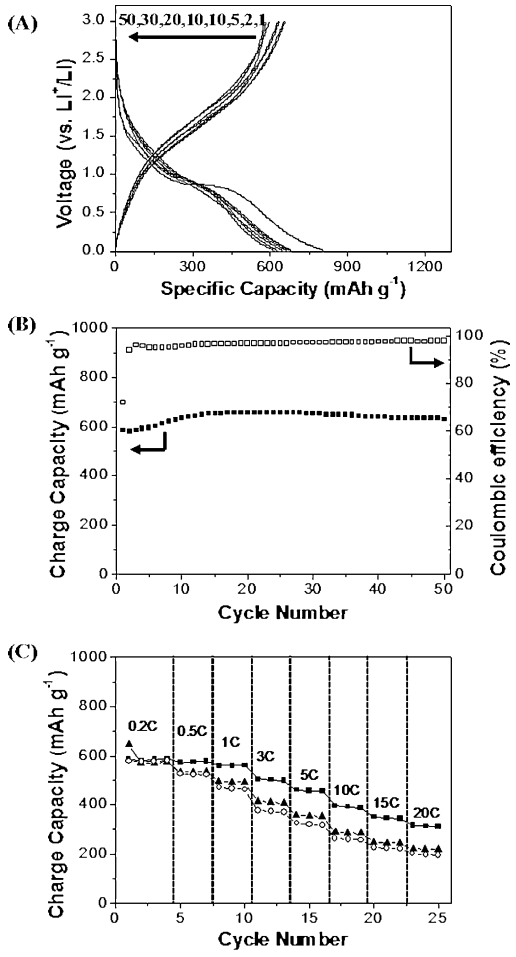

Figure 3. Electrochemical properties of CuO nanotube electrodes prepared from spin-coated Cu nanowires (C18-NH_2). (A) Voltage profiles of the CuO nanotube electrodes (1st, 2nd, 5th, 10th, 20th, 30th, and 50th cycle) at a rate of 0.1 C. (B) Cycling performance of the CuO nanotube electrodes at 0.1 C rate. (C) Rate capabilities of the CuO nanotubes prepared from CuO nanowires (C10-NH_2 (open circles), C14-NH_2 (solid triangles), and C18-NH_2 (solid squares)) at 0.2–20 C rates.

We furthermore found that the interconnection of CuO nanotube electrodes significantly enhanced the rate capability. Figure 3C shows the rate capabilities of the CuO nanotubes (made from C10-NH_2, C14-NH_2, and C18-NH_2) in the range of 0.2–20 C rates. As expected, the CuO nanotube electrode obtained from C18-NH_2 exhibited an excellent rate capability (316 mAh g^{-1} at a high rate of 20 C; capacity retention of 54% compared to 0.2 C rate). This result suggests that the CuO nanotubes with a smaller diameter (high surface area) effectively transfer an electron to the active materials, thus resulting in a significant enhancement of the discharging and charging rate.

In order to demonstrate the high-performance electrochemical properties of the CuO nanotube electrodes made from C18-NH_2, they were disassembled after cycling. Figure 4 shows the SEM images of the CuO electrodes before and after cycling. After 10 and 50 cycles, the diameter of the CuO nanotubes was increased through a volume change during cycling, due to the formation of solid-electrolyte interface (SEI) layers (Figure 4B,C). However, the morphologies of the CuO nanotubes after cycling are similar to that of the original CuO nanotubes before cycling. This result suggests that the CuO nanotubes adhere strongly to the SS current collector before and after cycles, thus leading

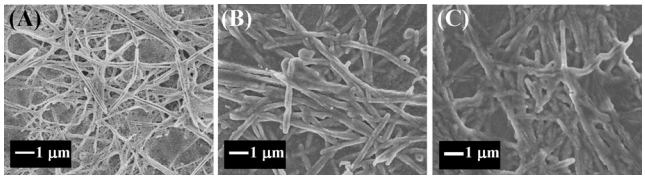

Figure 4. SEM images of CuO nanotube (C18-NH_2) electrodes (A) before cycling, (B) after the 10th cycle, and (C) after the 50th cycle. After cycling, the diameter of the CuO nanotubes was increased, but the morphologies of the CuO nanotubes was similar to that of the original CuO nanotubular structures.

to an excellent performance of the CuO electrode, including a high rate capability, a stable cycling, and a high reversible capacity.

In summary, we demonstrated a simple route for fabricating CuO nanotube electrodes by a thermal oxidation process of Cu nanowires spin-coated on a surface of SS foils. Since as-synthesized CuO nanotubes strongly adhered to the SS current collector, no binder or conductive materials were required. The nanotubular structure of CuO and interconnected CuO structures strongly bound to the SS foils, thus leading to significantly enhanced electrochemical properties, including a high reversible capacity (635 $mAh\,g^{-1}$), a highly stable cycling (capacity retention of nearly 100% after 50 cycles), and an excellent rate capability (315 $mAh\,g^{-1}$ at a high rate of 20 C). This strategy may provide an effective route that could be extended to other metal oxide materials.

Acknowledgements

This work was supported by the Converging Research Center Program through the Ministry of Education, Science and Technolgoy (2012K001251) and the WCU (R31-2008-000-20012-0) programs.

Keywords: copper · nanostructures · nanotubes · Kirkendall effect · lithium-ion batteries

[1] G.-A. Nazri, G. Pistoia, *Lithium Batteries: Science and Technology*, Kluwer Academic/Plenum, Boston, **2004**.
[2] J.-M. Tarascon, M. Armand, *Nature* **2001**, *414*, 359.
[3] M.-K. Song, S. Park, F. M. Alamgir, J. Cho, M. Liu, *Mater. Sci. Eng. R* **2011**, *72*, 203.
[4] C. Liu, F. Li, L.-P. Ma, H.-M. Cheng, *Adv. Mater.* **2010**, *22*, E28.
[5] P. G. Bruce, B. Scrosati, J.-M. Tarascon, *Angew. Chem.* **2008**, *120*, 2972; *Angew. Chem. Int. Ed.* **2008**, *47*, 2930.
[6] Y. Wang, H. Li, P. He, E. Hosono, H. Zhou, *Nanoscale* **2010**, *2*, 1294.
[7] H. B. Wu, J. S. Chen, H. H. Hng, X. W. Lou, *Nanoscale* **2012**, *4*, 2526.
[8] Z. Wang, L. Zhou, X. W. Lou, *Adv. Mater.* **2012**, *24*, 1903.
[9] Z. Wang, F. Su, S. Madhavi, X. W. Lou, *Nanoscale* **2011**, *3*, 1618.
[10] A. Débart, L. Dupont, P. Poizot, J.-B. Leriche, J. M. Tarascon, *J. Electrochem. Soc.* **2001**, *148*, A1266.
[11] F. Wang, W. Tao, M. Zhao, M. Xu, S. Yang, Z. Sun, L. Wang, X. Song, *J. Alloys Compd.* **2011**, *509*, 9798.
[12] M. Hasan, T. Chowdhury, J. F. Rohan, *ECS Trans.* **2009**, *19*, 3.
[13] J. Y. Xiang, J. P. Tu, L. Zhang, Y. Zhou, X. L. Wang, S. J. Shi, *J. Power Sources* **2010**, *195*, 313.
[14] Y. Hu, X. Huang, K. Wang, J. Liu, J. Jiang, R. Ding, X. Ji, X. Li, *J. Solid State Chem.* **2010**, *183*, 662.
[15] S. Ko, J.-I. Lee, H. S. Yang, S. Park, U. Jeong, *Adv. Mater.* **2012**, *24*, 4451.
[16] J. Liu, D. Xue, *Nanoscale Res. Lett.* **2010**, *5*, 1525.
[17] P. L. Taberna, S. Mitra, P. Poizot, P. Simon, J.-M. Tarascon, *Nat. Mater.* **2006**, *5*, 567.
[18] C. K. Chan, H. Peng, G. Liu, K. McIlwrath, X. F. Zhang, R. A. Huggins, Y. Cui, *Nat. Nanotechnol.* **2008**, *3*, 31.
[19] J. Packer, J. Vaughan, *A Modern Approach to Organic Chemistry*, Oxford, **1958**.
[20] Y. Chang, M. L. Lye, H. C. Zeng, *Langmuir* **2005**, *21*, 3746.
[21] D. Zhang, R. Wang, M. Wen, D. Weng, X. Cui, J. Sun, H. Li, Y. Lu, *J. Am. Chem. Soc.* **2012**, *134*, 14283.
[22] Y. Shi, H. Li, L. Chen, X. Huang, *Sci. Technol. Adv. Mater.* **2005**, *6*, 761.
[23] A. Swami, M. Kasture, R. Pasricha, M. Sastry, *J. Mater. Chem.* **2004**, *14*, 709.
[24] M. H. Cao, C. W. Hu, Y. H. Wang, Y. H. Guo, C. X. Cuo, E. B. Wang, *Chem. Commun.* **2003**, 1884.
[25] A. D. Smigelskas, E. O. Kirkendall, *Trans. AIME* **1947**, *171*, 130.
[26] Y. Yin, R. M. Rioux, C. K. Erdonmez, S. Hughes, G. A. Somorjai, A. P. Alivisatos, *Science* **2004**, *304*, 711.
[27] R. Nakamura, G. Matsubayashi, H. Tsuchiya, S. Fujimoto, H. Nakajima, *Acta Mater.* **2009**, *57*, 5046.
[28] H. J. Fan, M. Knez, R. Scholz, K. Nielsch, E. Pippel, D. Hesse, M. Zacharias, U. Gösele, *Nat. Mater.* **2006**, *5*, 627.
[29] J. G. Railsback, A. C. Johnston-Peck, J. Wang, J. B. Tracy, *ACS Nano* **2010**, *4*, 1913.
[30] M. Kaur, K. P. Muthe, S. K. Despande, S. Choudhury, J. B. Singh, N. Verma, S. K. Gupta, J. V. Yakhmi, *J. Cryst. Growth* **2006**, *289*, 670.
[31] R. Malini, U. Uma, T. Sheela, M. Ganesan, N. G. Renganathan, *Ionics* **2009**, *15*, 301–307.

Received: March 25, 2013
Published online: June 3, 2013